scientific reports

OPEN

Concomitant immunity to *M. tuberculosis* infection

Louis R. Joslyn[1,2], JoAnne L. Flynn[3], Denise E. Kirschner[2✉] & Jennifer J. Linderman[1✉]

Some persistent infections provide a level of immunity that protects against reinfection with the same pathogen, a process referred to as concomitant immunity. To explore the phenomenon of concomitant immunity during *Mycobacterium tuberculosis* infection, we utilized *HostSim*, a previously published virtual host model of the immune response following Mtb infection. By simulating reinfection scenarios and comparing with data from non-human primate studies, we propose a hypothesis that the durability of a concomitant immune response against Mtb is intrinsically tied to levels of tissue resident memory T cells (Trms) during primary infection, with a secondary but important role for circulating Mtb-specific T cells. Further, we compare *HostSim* reinfection experiments to observational TB studies from the pre-antibiotic era to predict that the upper bound of the lifespan of resident memory T cells in human lung tissue is likely 2–3 years. To the authors' knowledge, this is the first estimate of resident memory T-cell lifespan in humans. Our findings are a first step towards demonstrating the important role of Trms in preventing disease and suggest that the induction of lung Trms is likely critical for vaccine success.

The human immune system has the potential to respond effectively to infection with many pathogens. After a first encounter with a pathogen (primary infection) is cleared, immunological memory is typically protective against a second infection event (reinfection) at a later date. Some persistent pathogens (i.e. those that are not cleared) also confer protection against secondary infection[1–5]. This latter phenomenon, known as *concomitant immunity*, was first described in Stedman's medical dictionary as "infection-immunity"[6]. Formally, concomitant immunity is "the paradoxical immune status in which resistance to reinfection coincides with the persistence of the original infection"[7,8].

Concomitant immunity is thought to be pathogen-dependent and thereby mediated by different immune modalities depending on infection type. For example, persistent infection with lymphocytic choriomeningitis virus (LCMV) promotes a greater accumulation of relatively long-lived effector-like memory T cells at non-lymphoid sites[9]. In *Leishmania major* infection, relatively short-lived CD4 + regulatory T cells play a role in concomitant immunity by preventing total clearance of the pathogen during persistent infection[7] and it was recently found that if CD4 + effector T cells are not sustained, concomitant immunity against reinfection was inadequate[10]. Across multiple types of parasitic infections, separate and distinct cellular and antibody immune responses develop that are consistent with acquisition of concomitant immunity[1–5].

In tuberculosis (TB), which remains a significant global health crisis that was exacerbated by the COVID-19 pandemic, it is unclear if persistent *M. tuberculosis* (Mtb) infection in humans confers enduring protection against reinfection. The hallmark of TB, a primarily pulmonary disease, is the formation of lung granulomas: organized immune cellular structures that surround Mtb[11–14]. Granulomas are composed of various immune cells, including macrophages and T cells (primarily CD4 + and CD8 + T cells, although other unconventional T cell phenotypes and B cells are also present, reviewed in[15]). T cells have well-established critical functions against Mtb[16–20], but unlike other infections, T cells arrive approximately one month after primary infection[21]. The delays in lymph node T cell priming, activation, and trafficking through blood to lungs is characteristic of Mtb infection[22,23] and may be due to the slow growth of the bacilli and limited 'danger' signals[24] at early stages of infection during Mtb growth in the lungs[21].

Concomitant immunity against Mtb appears to provide at least some protection against reinfection. Observational cohort studies from natural infection case studies suggest that individuals with latent TB (LTBI – i.e., those who are persistently infected but are clinically asymptomatic) had a 35—80% lower risk of progression to active TB after re-exposure to Mtb compared to uninfected individuals[25–29]. In those studies, it was not possible

[1]Department of Chemical Engineering, University of Michigan, G045W NCRC B28, 2800 Plymouth Rd, Ann Arbor, MI 48109-2136, USA. [2]Department of Microbiology and Immunology, University of Michigan Medical School, 1150W Medical Center Drive, 5641 Medical Science II, Ann Arbor, MI 48109-5620, USA. [3]Department of Microbiology and Molecular Genetics, University of Pittsburgh School of Medicine, Pittsburgh, PA 15261, USA. ✉email: kirschne@umich.edu; linderma@umich.edu

1

to determine whether actual reinfection occurs, since active TB was the only outcome measure. Nonetheless, in a seminal study of nursing and medical students, those who were tuberculin skin test positive (TST +) and had LTBI were less likely to develop active TB during their years in hospital training than those who were TST negative[25]. Further, other studies in mice suggest that concomitant immunity is not fully protective against secondary infection with Mtb, but that bacterial burden from a secondary infection is reduced when compared to primary infection[30,31]. Cadena et al. showed that in non-human primates (NHP) concomitant immunity was robust against a secondary infection with Mtb[32]. However, due to the inherent constraints of NHP studies, Cadena et al. were unable to conduct re-exposures at multiple time points after primary infection and therefore were unable to quantify the potential longevity of a concomitant immune response. Based on the observation that Mtb-specific T cells reside in uninvolved lung tissue prior to reinfection, Cadena et al. hypothesized that resident memory T cells prevent the establishment of reinfection.

The defining feature of lung resident memory T cells (Trms) is their persistent residence within nonlymphoid tissues and inability to circulate through blood stream and lymphatics[33]. These cells act as a sentinel against future infection and have been shown to be protective against infections with influenza virus, herpes simplex virus, and human immunodeficiency virus (reviewed in[33]). Further, skin CD69 + Trm cells have been shown to provide concomitant immunity in the case of cutaneous leishmaniasis[34]. Relatively few studies have examined Trms in the context of TB[35]. However, mucosal administration of the BCG vaccine in mice, as well as adoptive transfer of CD8 + Trms, have demonstrated enhanced protection against Mtb, presumably through the ability of Trm (defined in these studies by CD103 + and CD69 + surface marker expression) to respond quickly following infection (studies reviewed in[36]). Additionally, intravenous administration of BCG in NHPs provided robust protection against infection, and BCG IV vaccinated NHP had high levels of CD69 + Trm in lungs in contrast to intradermal or aerosol BCG vaccinated NHP[37]. In general, Trms are thought to develop during the adaptive immune response to primary Mtb infection and have been identified within uninvolved lung tissue of infected hosts[32]. However, experimental studies have so far been unable to define their role in concomitant immunity against Mtb and the longevity of this cell population in the lung has not been well-characterized in NHPs or humans.

As a complementary approach, mathematical and computational modeling can predict mechanism and timing of major immune events beyond the timeline of experimental studies. In TB, modeling has been used to explore various aspects of granuloma formation[38,39], drug-dynamics[40,41], and immune cell and cytokine dynamics within lung granulomas[39,42–44]. The advantages of a modeling approach are well-suited to answer outstanding questions about reinfection and the potential longevity of Trm cell populations in the human lung.

We previously calibrated and validated *HostSim*, a whole-host modeling framework that captures key elements of TB immune responses and pathology across lungs, lymph nodes and blood[45], using multiple datasets derived from published NHP studies and have shown the ability of this model to capture heterogeneous host-scale clinical outcomes such as infection clearance, control (LTBI) or active disease. Here we used the *HostSim* framework to address two outstanding questions about Trms and concomitant immunity in TB: Do Trms mediate concomitant immunity in Mtb? Can we predict the lifespan of Trms in primate lung tissue and therefore the duration of concomitant immunity against Mtb infection?

Results

Resident memory T cells (Trm) are the main mediators of concomitant immunity against Mtb reinfection.

In NHPs, ongoing primary infection with Mtb confers protection against reinfection 16 weeks later[32]. Four weeks after the secondary inoculation, animals were necropsied and granuloma bacterial burdens from both primary and secondary inoculation events were obtained. By sampling the parameter space of *Host-Sim*, we created a population of 50 virtual hosts and simulated the virtual hosts following the NHP experimental protocol (Fig. 1A). We have previously compared in silico granuloma CFU levels to the NHP in vivo granuloma CFU levels from primary infection[45]. Below, we compare in silico and in vivo granuloma reinfection CFU levels.

We added Trms to our *HostSim* modeling framework due to their potential role in mediating protection against reinfection (see Methods, section *Including resident memory T cells during reinfection in HostSim* for details about this cell population within *HostSim*). With the addition of Trms into *HostSim*, we observe that concurrent Mtb infection limits the establishment of reinfection granulomas, matching observed reinfection dynamics in NHPs[32]. We predict that the vast majority of reinfection granulomas are sterilized prior to 28 days post-infection using *HostSim* (Fig. 1). Our simulations resulted in virtual hosts where reinfection was not established, i.e. no granulomas due to secondary challenge were detected (Fig. 1B) and virtual hosts where secondary challenge resulted in granulomas (Fig. 1C) (gray lines indicated reinfection granuloma CFU). For 33 out of the 50 virtual hosts, reinfection was not established, as these hosts had total sterilization of all reinfection granulomas prior to day 28. This is consistent with the NHP study, which showed 5 of 8 monkeys had total sterilization of reinfection granulomas at this same time point. If we re-simulate the 50 virtual hosts but delete (knockout, KO) Trms, we no longer match the NHP dataset. Intriguingly, reinfection granulomas in the KO study still contained significantly lower bacterial burdens (~ fivefold less) than primary infection granulomas (Fig. 1D, red data points). This suggests that while Trms are the main drivers of a concomitant immune response, additional immune cells also likely affect the growth of bacteria within reinfection granulomas. Additionally, components of the immune system that were not included in *HostSim* such as unconventional T cells or antibodies against TB, may play a role in reinfection granuloma environments.

Predicting the lifespan of Trms and durability of concomitant immunity.

While concomitant immunity is protective against reinfection at 112 days in NHPs, the duration of a concomitant immune response over time is not yet known[32]. However, prospective cohort studies from the pre-antibiotic era of TB treatment
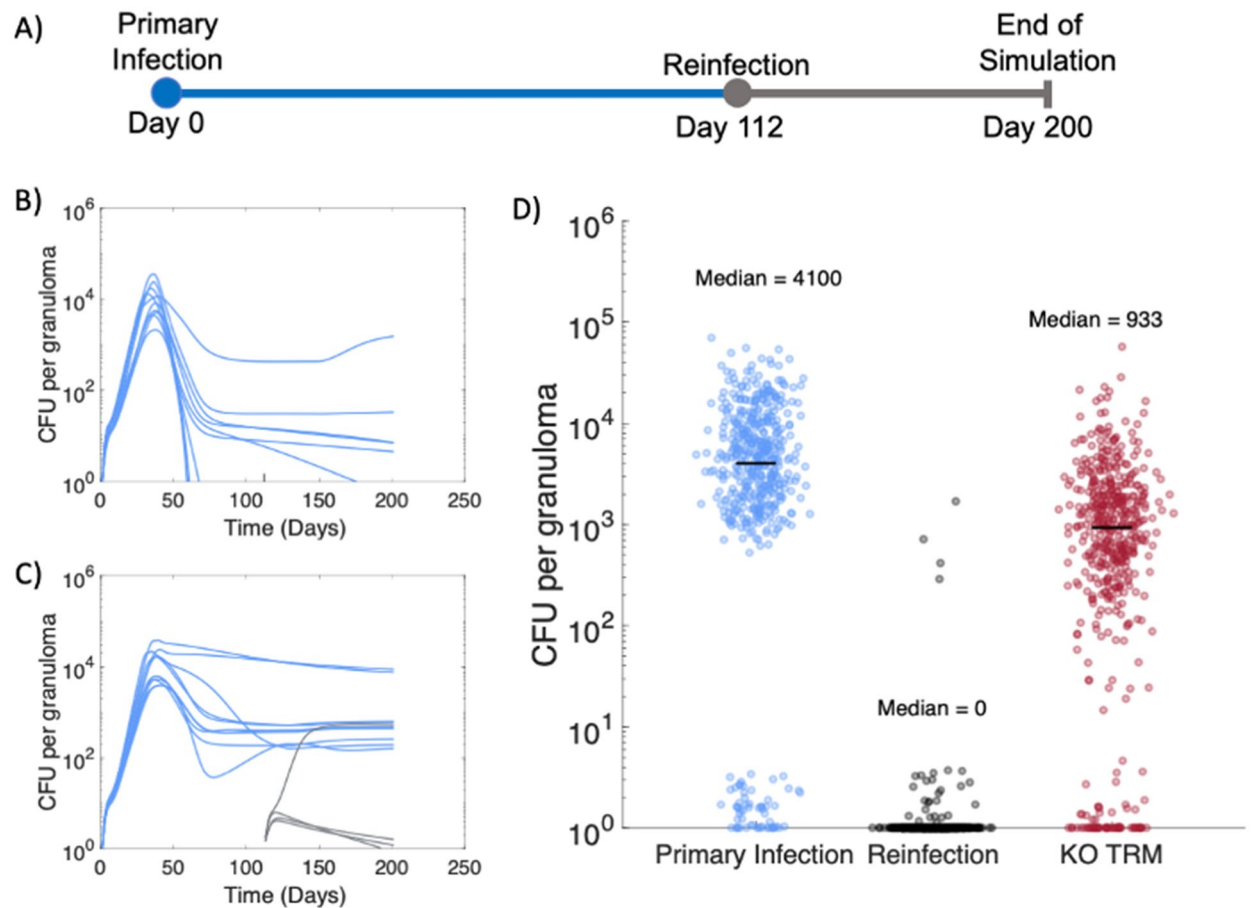
Figure 1. Resident memory T cells protect against establishment of reinfection granulomas in virtual population of 50 hosts. (**A**) Experimental protocol for reinfection study. Primary infection (blue) with 10 CFU inoculum occurred at day 0 and reinfection (gray) with 10 CFU inoculum occurred at day 112, matching the NHP study protocol[32]. Granuloma CFU trajectories from two representative hosts shown in panel (**B**) & (**C**). (**D**) Across 50 virtual hosts, reinfection granulomas exhibit greater sterilization compared to primary infection granulomas 28 days post-infection, as previously observed in NHPs[32]. We re-simulated the same 50 hosts but "knocked-out" (KO) the Trm cell population at reinfection (red data points). CFU per granuloma between KO Trm virtual hosts and the primary infection granuloma CFU was significantly different (Vargha and Delaney's A measure = 0.76).

predict that individuals with latent Mtb infection (Tuberculin-skin test positive, asymptomatic, infected for an undetermined period of time, spanning years) had a 79% reduced risk of developing active TB following re-exposure to Mtb compared to uninfected individuals[25]. These studies were observational, and it was not possible to determine the exact time of initial infection or re-exposure as the only outcome measure was active TB cases. However, these studies provide an opportunity for a case study: we can use *HostSim* to predict the lifespan of lung Trm—which our in silico knock-out experiment (Fig. 1D) predicts as a major contributor to concomitant immunity.

We performed three sets of virtual reinfection studies using the same 500 virtual hosts (see Methods) to predict the lifespan of lung Trms and measure longevity of a concomitant immune response in *HostSim*. We alter the death rate of lung Trms between the three sets of reinfection studies to predict Trm lifespan in primates.

To estimate the lifespans of Trms during TB, we classify hosts across our virtual populations as active, latent or Mtb eliminators following reinfection to identify which Trm lifespan best aligns with the results of the human cohort study[22]. To this end, we display the breakdown of active TB (dark blue), LTBI (green) and Mtb eliminator (yellow) cases (as defined by the total lung bacterial burden [Supplementary Fig. S1]) at day 200 post-reinfection for the 500 virtual hosts across 21 reinfection studies (Fig. 2). When the lifespan of Trms is set to previous estimates in mice proposed from Morris et al. ($d_{Trm} = 0.03$ cells/day)[46], concomitant immunity wanes quickly (Fig. 2A, D). In contrast, if the lifespan of Trms lasts for multiple decades ($d_{Trm} = 0.0001$ cells/day; Fig. 2C, F), all virtual hosts sterilize or control reinfection. Each of these Trm lifespans result in predictions that are inconsistent with the human cohort studies. Only when the lifespan of Trms is ~ 25 × longer than originally estimated by Morris et al. ($d_{Trm} = 0.0012$ cells/day, calculated based on allometric scaling between humans and mice), does the reduced risk of active TB align with that of the human cohort studies (Fig. 2B, E). Across the 21 reinfection studies in Fig. 2B, the average reduced risk of active TB is 77% following reinfection. This is a prediction that is
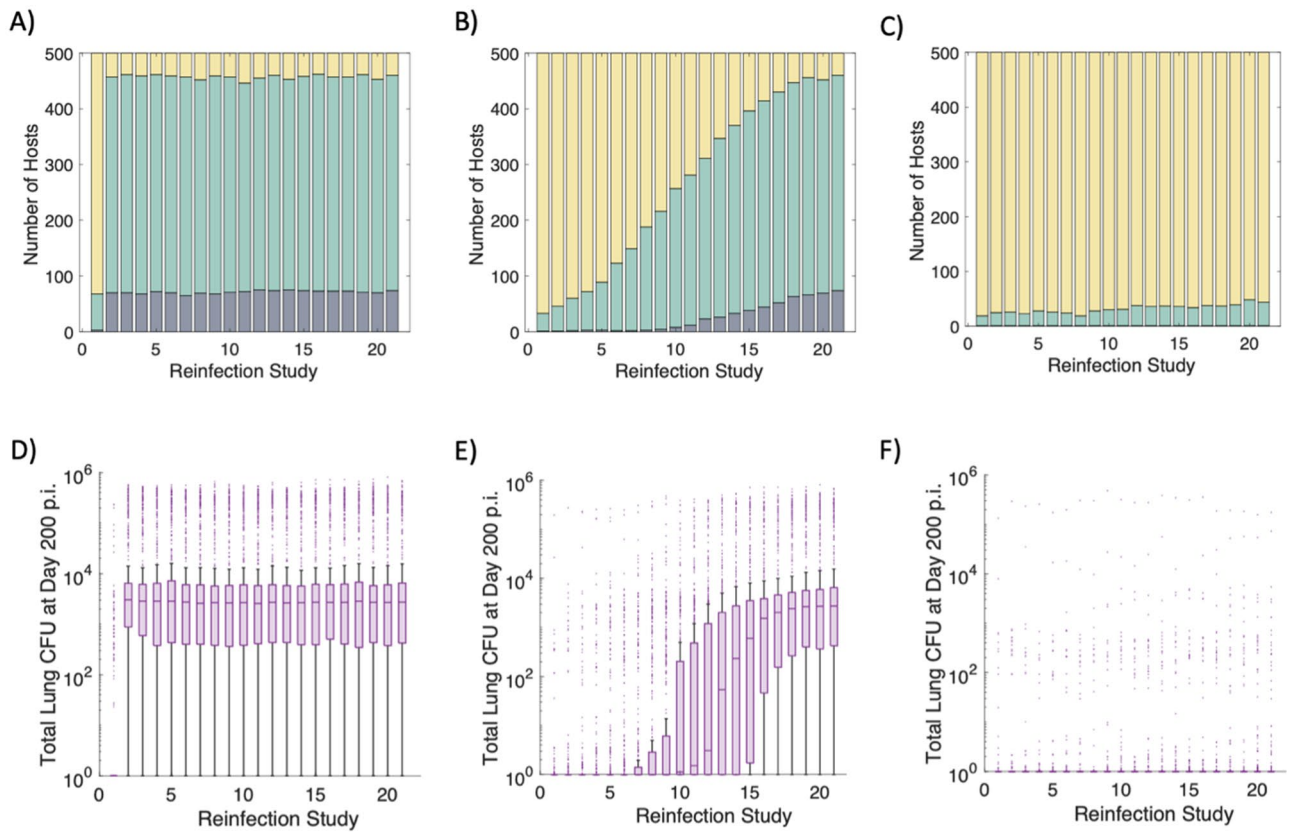
Figure 2. Clinical classifications and total lung CFU across three sets of virtual reinfection studies. Clinical classifications for 500 virtual hosts across 21 separate reinfection studies when the lifespan of Trms is varied from 33 days, 833 days, or 10,000 days (d_{Trm} = 0.03, 0.0012, or 0.0001 cells/day) (**A**, **B**, **C**, respectively). Each stacked bar chart shows the breakdown of active TB (dark blue), LTBI (green) or Mtb eliminator (yellow) hosts for each reinfection study. Clinical classifications are determined according to total lung CFU 200 days after reinfection. Box-and-whisker plots show the distribution of total lung CFU across the 500 virtual hosts for each reinfection study when d_{Trm} = 0.03, 0.0012, or 0.0001 cells/day (**D**, **E**, **F**, respectively).

consistent with reduced risk estimates in humans (~ 79%, Andrews et al.[25]). Thus, we predict that the lifespan of an individual Trm is approximately 2–3 years.

Mtb-specific blood T cells from primary infection offer protection against active TB during reinfection in absence of Trm populations. Using *HostSim* we showed that concomitant immunity is intrinsically associated with Trm lifespan (Figs. 1 and 2). Intriguingly, at reinfection timepoints after the majority of Trm cells have died, we still note an average reduction of ~ 35% in active TB from reinfection compared to controls who were only infected once (Fig. 2A, reinfection studies 2–21). We use these reinfection studies to identify mechanisms driving active TB following reinfection events that may occur after waning of Trm populations.

In Fig. 3, we focus on the first set of reinfection studies, when the life span of Trms is 33 days (d_{Trm} = 0.03 cells/day), although the results herein are consistent across the three sets of reinfection studies (Supplementary Fig. S3). In the first set of reinfection studies, the Trm population is no longer present by reinfection timepoint 212 days after primary infection (Fig. 3A). For reinfection study numbers 2–21, we observed that the majority of virtual hosts still control infection, and are classified as LTBI, even without the presence of Trm populations in the lung (Fig. 3A). Further, we observed that virtual hosts who control reinfection had higher counts of Mtb-specific effector memory (Fig. 3B), effector (Fig. 3C), and central memory (Fig. 3D) T cells one day prior to reinfection as compared to hosts that went on to develop active TB after reinfection. Thus, we predict that the numbers of Mtb-specific T cells in the blood prior to reinfection is a key factor for protection against active TB following reinfection in the absence of Trms.

Discussion

Concomitant immunity is a special case of immune memory that is generated when a host is re-exposed while they are currently harboring a primary infection by the same pathogen. However, concomitant immunity does not provide a robust and enduring immune response against reinfection for all persistent pathogens[47]. For example, during chronic HIV infection, reinfection has been shown to clinically arise as early as one-year after primary infection[48]. If a concomitant immune response is observed, then the cellular-mediators and longevity of
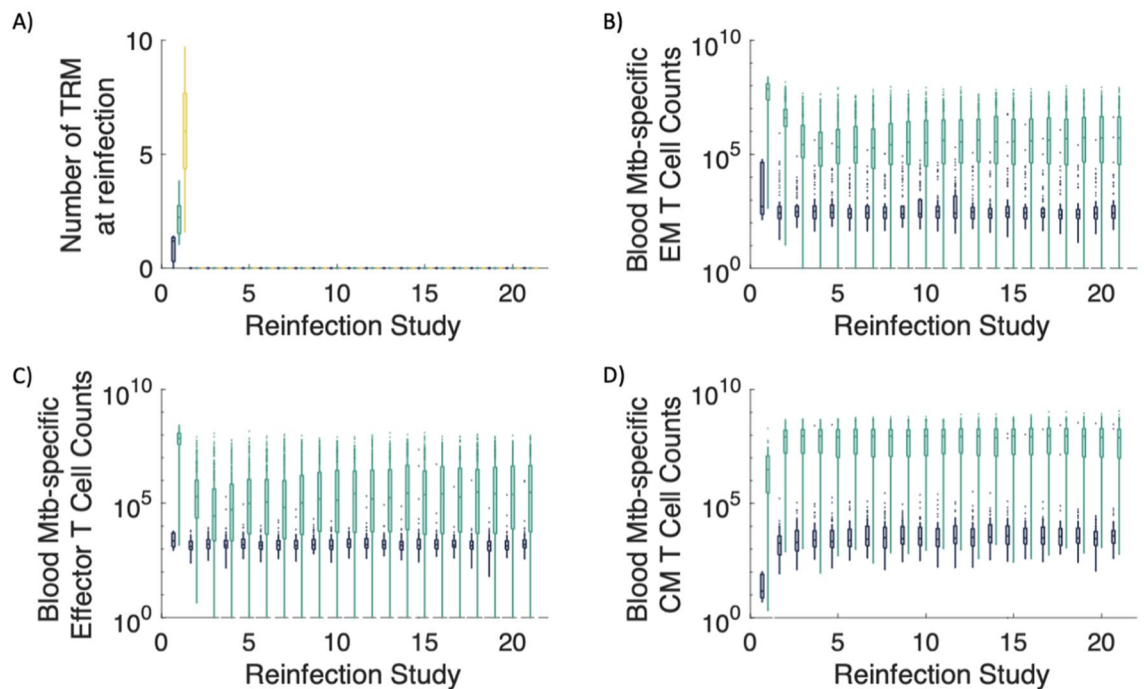
Figure 3. In the absence of Trms, Mtb-specific T-cell counts in blood delineate active vs. LTBI outcomes following reinfection. (**A**) In our first set of reinfection studies, we set the lifespan of Trms to be 33 days (d_{Trm} = 0.03 cells/day), and the Trm population wanes by day 212, the reinfection time point of reinfection study 2. Box-and-whisker plots show the distribution of Mtb-specific effector memory (EM), effector, and central memory (CM) T cell counts in the blood one day prior to the timepoint of reinfection for each reinfection study (**B**, **C**, **D**, respectively). We stratify the T-cell numbers according to a host's total lung CFU at a time point 200 days later. If a virtual host was classified as an active TB case (total lung CFU > 10^5), the box and whisker plot is dark blue. If the virtual host was classified as an LTBI case (total lung CFU < 10^5), the box and whisker plot is green. Note that the vast majority of LTBI virtual hosts have larger numbers of Mtb-specific blood effector, effector memory and central memory T cells than that of their active TB case counterparts.

immunity appear to be pathogen-dependent, ranging from memory T cell mediated immunity in chronic LCMV to extremely short-lived immunity in parasitic infection[7,9,10]. In TB, concomitant immunity against reinfection appears protective, but the longevity and cellular mediators of such a response are not yet known.

To address these uncertainties, we utilize *HostSim*, our novel mathematical and computational model that captures the dynamics of Mtb infection in a primate host at a whole-host scale. Briefly, HostSim includes lung, lymph node, and blood compartments, and tracks whole-host scale outcomes such as the total number of lung granulomas; all key compartments and outcomes for pulmonary TB. We use *HostSim* to directly investigate the cellular mechanisms that lead to concomitant immunity by relating events and dynamics within each individual virtual host to population scale outcomes. A significant benefit of this systems biology approach is that the group of 500 virtual individual *HostSim* simulations is identical across reinfection studies. Therefore, we can directly compare each reinfection study against the others. This allows us to build on the studies begun in NHP[32] and perform simulated studies impossible to do with in vivo experiments. Our predictions add support to growing evidence[25,32] that primary Mtb infection provides a concomitant immune response against reinfection. Further, we propose a hypothesis that the longevity of concomitant immunity against Mtb is intrinsically tied to the magnitude of numbers of Trm cells generated, as our studies indicate that these cells are key mediators of protection against reinfection.

Trms offer intriguing targets for vaccination. In fact, intravenously administered BCG was recently shown to provide a pool of lung Trms that exhibited protection against infection with Mtb in NHPs[37]. The longevity of these cells has implications for vaccine design. In humans, the longevity of Trms in the lungs is not yet known. In this work, we create a very simple model of Trms where we assume there is some level of them present in the lung after a long Mtb infection, and then allow them to decay due to a lifespan over time. This allows us to predict that in the context of an ongoing, persistent Mtb infection, the upper bound lifespan ($1/d_{Trm}$) of Trms within the lungs is approximately 2 to 3 years. To our knowledge, this is the first estimate of Trm lifespan in human lungs and contributes to growing evidence that this long-lived cell population can persist > 1 year[49]. Note that this is likely an overestimate of the lifetime; it is likely that Trms continue to be generated throughout a persistent infection and thus a shorter lifetime would be sufficient to account for the data. The creation of a mechanistic mathematical model of Trms during TB together with NHP datasets is the subject of ongoing studies in our groups.

Our findings suggest that if immunity can only be achieved through an antigen-specific Trm cell population, then a successful vaccine must extend the durability, magnitude or longevity of this cell population, thereby toggling the properties of T cell memory across time. Macaque studies with a CMV vector-based TB vaccine

suggest that this vaccine platform might provide the necessary antigen persistence for continuous stimulation toward a protective memory T-cell pool across time[50]. However, vaccine protection studies in NHPs have yet to be completed where the timing of infection was > 1 year after vaccination[50].

In the absence of Trm populations, we still note limited protection against reinfection (Figs. 1D and 3). In our first set of reinfection studies, the average reduction of risk of developing active TB was 35% for reinfection study numbers 2–21 (the studies that included a reinfection timepoint after the loss of all lung Trms). This percentage is consistent with estimates of protection from reinfection in a household contact study in Peru, that showed 3–35% protection against reinfection across an average interval of 3.5 years[29]. Our works suggests that in addition to Trms, there are other mechanisms within the body to prevent uncontrolled bacterial growth following reinfection and perhaps this is reflected in the study of Peruvian individuals. We posit that individuals develop active TB following reinfection due to inadequate adaptive immune responses where the magnitude of both Trms and circulating Mtb-specific T cells must be insufficient.

In this study, we could not model every cell type present in both primary infection and reinfection granulomas. For example, unrestricted or unconventional T cells have not been considered in this work but could influence reinfection granuloma environments and have important implications for vaccination[15]. These cell types (as well as others) could be considered in future work. Additionally, our simulations to determine Trm lifespan based on natural TB case studies in humans assumes translatability between NHP and patient simulations using *HostSim*. Potentially, mechanisms of prevention against reinfection could differ between NHP and humans, although data is limited to better inform these assumptions. Finally, while natural TB case studies have shown protection against reinfection[25,28,29], patients who successfully complete TB drug treatment are at an increased risk of developing TB upon reinfection, with an incidence rate four times that of primary infection[51,52]. We do not capture this population in the current study, although current work in our group is incorporating drug treatment into *HostSim* and could further investigate this phenomenon.

Methods

The HostSim modeling framework.
Recently we presented *HostSim,* a whole host computational and mathematical modeling framework of Mtb infection[45]. Briefly, *HostSim* is a hybrid, multi-scale model that links ordinary differential equations (ODEs) at the cellular and cytokine scale to outcomes at the whole-host scale, like total bacterial burden in the lung or cellular dynamics across the lymph nodes and blood. *HostSim* tracks the development of multiple lung granulomas, as well as immune cell trafficking to the lymph node and from the blood. Within the lungs, each granuloma is an agent that is placed stochastically within the boundary of a 3-dimensional lung environment. Within each lung granuloma, *HostSim* captures the dynamics of different cytokines, immune cells, and bacterial concentrations across time. Each granuloma captures the impact of innate and adaptive immune responses against Mtb. To describe innate immunity within a granuloma, we track populations of resting macrophages, infected macrophages, and activated macrophages. To capture the impact of the adaptive immune system, we describe primed CD4 + and CD8 + T cell populations. Following known biology, primed CD4 + T cells differentiate into effector Th1 or Th2 cell populations and primed CD8 + T cell populations differentiate into cytokine producing or cytotoxic CD8 + T cell populations. Additionally, each granuloma contains pro-inflammatory and anti-inflammatory cytokines. These include IFN-γ, TNF-α, IL-10, IL-4 and IL-12.

We additionally describe the initiation of adaptive immunity within a lymph node (LN) compartment after receiving signals from antigen presenting cells that migrate from the lungs. In the LN model, which has been previously presented[45,53,54], we track specific and non-specific CD4 + and CD8 + naïve, effector, effector memory, and central memory T cell responses using a compartmentalized system of 31 non-linear ordinary differential equations. Finally, we track immune cell counts within a blood compartment that acts as a bridge between lymph nodes and lungs. Effector and effector memory T cells are recruited from the blood into the lung granuloma environment according to the inflammatory profile of each granuloma.

The in silico hosts that are created during our simulations are comprised solely of lungs, LN and blood. We focus *HostSim* on these sites that are known to be associated with pulmonary TB for this study, but we believe the results are without loss of generality: other organs involved in extrapulmonary TB cases (such as liver or brain) could be added to fine tune our predictions on other clinical outcomes of TB which may or may not be associated with a concomitant immune response against reinfection. See Supplementary Materials for new equations and details that were added to *HostSim* during this work. Additionally, see our dedicated *HostSim* website for details of *HostSim,* equations, pseudo-code and movies of infection simulations: http://malthus.micro.med.umich.edu/lab/movies/HostSim/.

Virtual hosts and TB outcomes.
Using *HostSim,* we sample parameter space to create a virtual population of hosts and use it to delineate TB outcomes across this virtual host population. In this work, and similar to previous work[45], we identify Mtb eliminators, whose total lung CFU < 1, active TB cases, whose total lung CFU > 10^5, and LTBI, all other virtual hosts following infection. Supplementary Fig. S1 displays the breakdown of each clinical classification following primary infection, wherein across 500 virtual hosts, 110 are classified as active TB cases, 366 are classified as LTBI cases, and 24 are classified as Mtb eliminators.

Including resident memory T cells during reinfection in HostSim.
To test the proposed role of Trms in concomitant immunity, we expanded *HostSim* to include this cell population. To do this, we have two key assumptions about the roles of Trms during reinfection. First, Trms have been shown to kill pathogens upon re-encounter very quickly, presumably by rapidly activating macrophages to kill their intracellular bacteria[32,33,36]. Therefore, we assume that Trms in *HostSim* assist infected macrophages in killing intracellular bacteria at a rate proportional to bacteria, macrophage, and Trm counts within the granuloma.
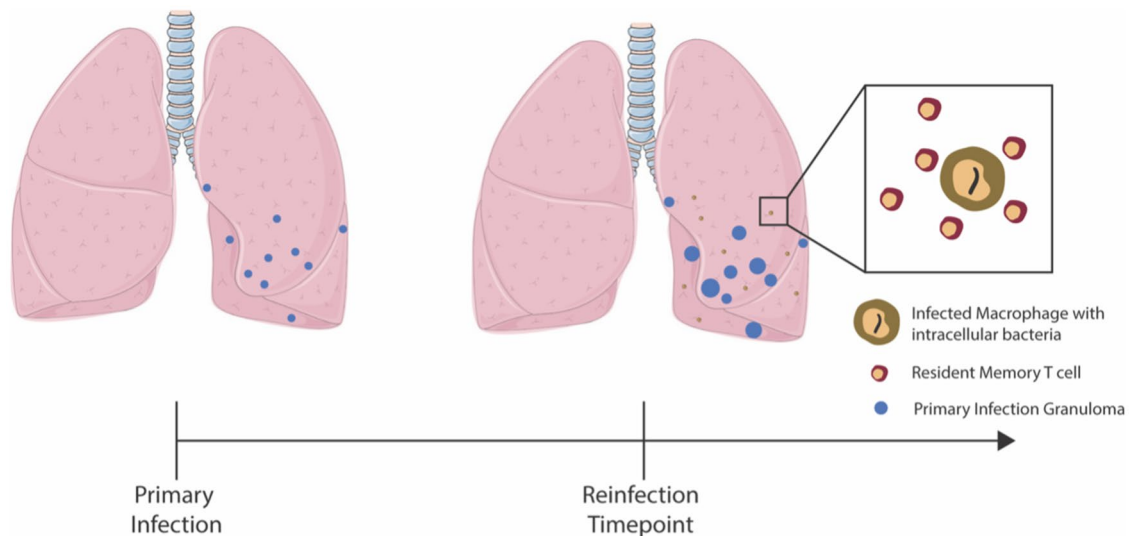
Figure 4. Resident Memory T cells impact establishment of reinfection. Primary infection begins with the inoculation of 10 CFU. At the reinfection timepoint, which varies from study to study, virtual hosts are re-inoculated with 10 CFU. Trm numbers vary at the time of reinfection depending on the Trm lifespan and the reinfection timepoint of the virtual study.

Second, Mtb-specific Trms have been identified in uninvolved lung tissue during primary infection[32]. Thus, we assume Trms would be present at very early stages prior to granuloma formation upon reinfection. To identify how many Trms might be present, we compare the reinfection CFU dynamics from the NHP study[29] at the reinfection timepoint (day 112) and use 1 to 10 Trm as initial conditions (Figs. 1 and 4). However, when we perform the parallel virtual reinfection studies (see below), we change the initial condition of the Trm population to reflect the lifespan of this cell population (see Trm lifespan section below). Based on these assumptions, we expanded the set of granuloma ordinary differential equations in *HostSim* to include an equation for Trms during reinfection scenarios (Fig. 4). (See supplement for equations).

Resident memory T cell (Trm) lifespan in the lungs. The lifespan of lung Trm in humans is largely unknown, but there is evidence that Trm populations are not as stable in the lung environment as they are in the skin or other locations[55,56]. Morris et al. used an exponential decay function to model the longevity of Trm populations across time and assumed no influx to the lung Trm population:

$$T_{RM} = T_{RM}(0)e^{d_{TRM}t}$$

where d_{TRM} is the death rate of Trm[46]. By calibrating to mice lung Trm datasets, Morris et al. determined $d_{TRM} = 0.03$ cells/day, or a lifespan of about 33 days (where lifespan is calculated as $1/d_{Trm}$). As they note, human lung Trms are less well-studied, primarily due to inability to sample healthy lung tissue. In our parallel virtual host reinfection studies (see below), we utilize this Trm longevity function to inform the initial conditions of Trms in reinfection scenarios. Additionally, we test different values for Trm death rates to predict the lifespan of these cell types in primates.

Reinfection events in HostSim. Reinfection studies within *HostSim* involve re-inoculating our virtual hosts with 10 CFU at the reinfection timepoint, which seeds 10 unique new granulomas within the lung environment (Fig. 4). Each reinfection granuloma begins with one intracellular bacterium, one infected macrophage and between 1 and 10 Trms as initial conditions.

Parallel virtual host reinfection studies. To predict the lifespan of Trms in the lung, we perform several parallel virtual host studies. Figure 5 demonstrates the experimental protocol for three sets of 21 reinfection studies. Each reinfection study consists of the same 500 individual *HostSim* simulations run for 500 virtual hosts over approximately a 7-year timeframe (2,500 total days) differing only in the time of reinfection. Study 1 begins with a reinfection timepoint at day 112 (the reinfection timepoint used in the NHP dataset from Cadena et al.[32]) and each subsequent study has a reinfection time point occurring 100 days after the previous study.

The 21 reinfection studies are each simulated three times, varying the death rate of Trms between each set. The first death rate, 0.03 cells/day, is the predicted death rate of Trm in mice from Morris et al.[46]. The second, 0.0012 cells/day, was calculated based on allometric scaling, as we assume humans live ~ 25 × longer than mice[57]. The third death rate selected was 0.0001 cells/day, a rate similar to that observed for central memory T cell populations, which are known to persist for decades[58].
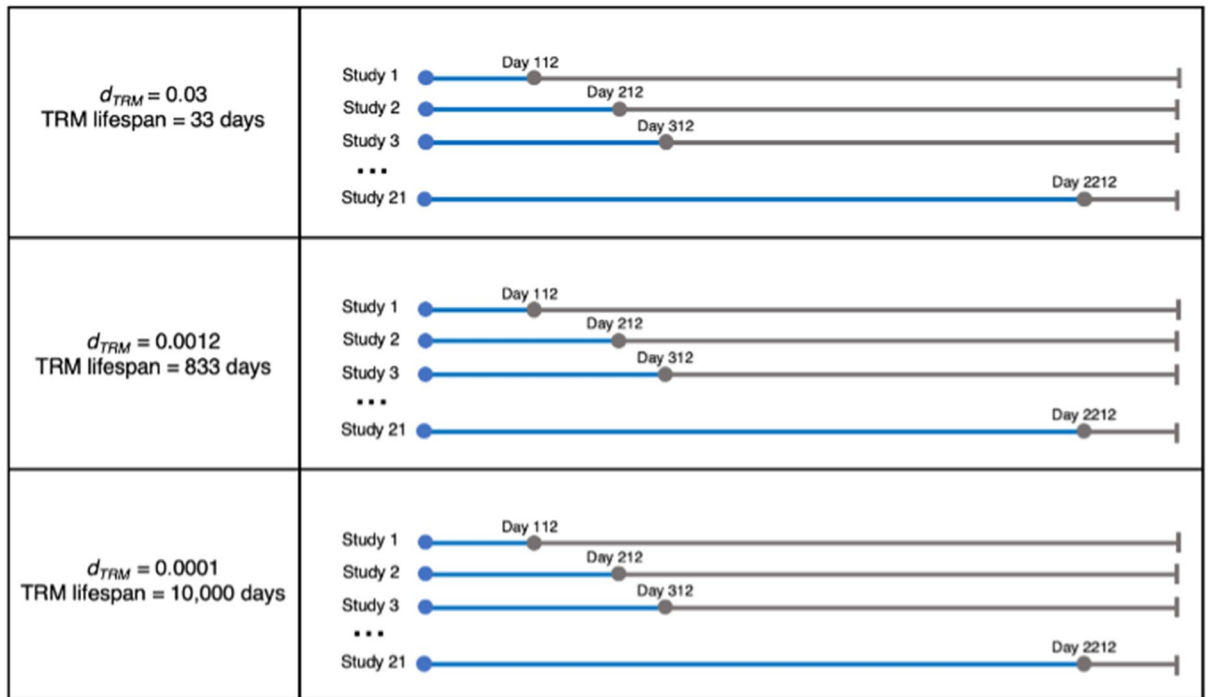
Figure 5. Parallel virtual host reinfection studies to predict Trm lifespan. The experimental protocol for our *HostSim* reinfection studies. We performed 3 sets of 21 separate reinfection studies on 500 virtual hosts, where the only difference between studies was timing of Mtb reinfection with a low dose of 10 CFU. Reinfection time points shown as gray dots on the timeline, wherein reinfection time points were simulated 100 days apart for each of the 21 studies, beginning at day 112 for Study 1 and ending with reinfection occurring at day 2212 for Study 21. In the first panel, we show the assigned different death rates of Trm (d_{Trm}) for each of 3 sets of reinfection studies. In total, we perform 63 reinfection studies where the same 500 hosts are simulated for 2500 days (approx. 7 years).

Calculating reduced risk of active TB following reinfection compared to primary infection.

Studies from the pre-antibiotic era of TB tracked the percentage of nursing students that contracted active TB disease[25]. Upon entering nursing school, students were stratified into two groups: those that had a positive Tuberculin Skin Test (TST), indicating previous exposure to Mtb, and those that had a negative TST, indicating no previous exposure to Mtb. A meta-analysis of these studies showed that individuals with a TST+ upon entering nursing school were at a 79% reduced risk of developing active TB compared to TST- individuals[25]. Assuming that all nurses had similar exposure to infectious TB patients, these studies are strong evidence of a protective concomitant immune response against reinfection. Supplementary Fig. S2 shows the data from these studies – note that studies with a longer period of observation (closer to 5 years) saw greater percentages of active TB cases among the TST+ population compared to those where students were observed for two years or less. Although this association is not statistically significant, the greater percentage of active TB cases during longer studies suggests a potentially waning protection from concomitant immunity.

Using *HostSim,* we can estimate the reduced risk of developing active TB from reinfection for virtual hosts. We do this by simulating a virtual population of hosts and comparing 1) the fraction of virtual hosts which develop active TB from primary infection and 2) the fraction of virtual hosts which develop active TB from reinfection. These two fractions are analogous to the TST- and TST+ groups in the meta-analysis of nursing students, respectively[25]. As Supplementary Fig. S1 shows, 110 out of a virtual population 500 hosts will develop active TB (total lung CFU > 10^5 at day 200 post-infection) following primary infection. This number (110/500) acts as our expected value following infection. We determine the second fraction during our reinfection studies by counting the number of hosts that have a total lung CFU > 10^5 at 200 days after reinfection. As an example, if 50 out of 500 virtual hosts develop active TB after reinfection, the risk reduction calculation would be as follows (in absolute value):

$$\frac{observed - expected}{expected} = \left| \frac{\begin{array}{c}\text{fraction of active hosts} \\ \text{following reinfection}\end{array} - \begin{array}{c}\text{fraction of active hosts} \\ \text{following primary infection}\end{array}}{\begin{array}{c}\text{fraction of active hosts} \\ \text{following primary infection}\end{array}} \right| = \left| \frac{\frac{50}{500} - \frac{110}{500}}{\frac{110}{500}} \right|$$

resulting in a 54.5% reduced risk of developing active TB.

Model environment and analysis. Model code and preliminary data analysis is written in MATLAB (R2020b). ODEs are solved using MATLAB's ode15s stiff solver. Simulation for a single in silico individual across 200 days post-infection can be performed on an 8-core laptop in approximately 30 s. Bash scripts were written for submission to run on the Great Lakes HPC Cluster at the University of Michigan for parallel virtual host reinfection studies. Post-processing statistical analysis and graphing was performed in MATLAB (R2020b).

Data availability

All data generated or analyzed during this study are included in this published article and are available upon request to the corresponding authors.

References

1. Buck, J. C., de Leo, G. A. & Sokolow, S. H. Concomitant immunity and worm senescence may drive schistosomiasis epidemiological patterns: An eco-evolutionary perspective. *Front. Immunol.* **11**, 160 (2020).
2. Miller, H. M. & Gardiner, M. L. Passive immunity to infection with a larval tapeworm of the albino rat. *Science* **75**(1940), 270 (1932).
3. Mitchell, G. F. A note on concomitant immunity in host-parasite relationships: A successfully transplanted concept from tumor immunology. *Adv. Cancer Res.* **54**, 319–32 (1990).
4. Lightowlers, M. W. Fact or hypothesis: Concomitant immunity in taeniid cestode infections. *Parasite Immunol.* **32**, 582–9 (2010).
5. MacDonald, A. J. *et al.* Differential cytokine and antibody responses to adult and larval stages of Onchocerca volvulus consistent with the development of concomitant immunity. *Infect. Immun.* **70**(6), 2796–2804 (2002).
6. Stedman, T. L. *Stedman's medical dictionary for the health professions and nursing* (Lippincott Williams Wilkins, 2005).
7. Belkaid, Y., Piccirillo, C. A., Mendez, S., Shevach, E. M. & Sacks, D. L. CD4+CD25+ regulatory T cells control Leishmania major persistence and immunity. *Nature* **420**(6915), 502–507 (2002).
8. Belkaid, Y. & Tamoutounour, S. The influence of skin microorganisms on cutaneous immunity. *Nat. Rev. Immunol.* **16**, 353–66 (2016).
9. Beura, L. K. *et al.* Lymphocytic choriomeningitis virus persistence promotes effector-like memory differentiation and enhances mucosal T cell distribution. *J. Leukoc. Biol.* **97**(2), 217–25 (2014).
10. Peters, N. C. *et al.* Chronic parasitic infection maintains high frequencies of short-lived Ly6C+CD4+ effector T cells that are required for protection against re-infection. *PLoS Pathog.* **10**(12), 160 (2014).
11. Flynn, J. L., Gideon, H. P., Mattila, J. T. & Lin, P. L. Immunology studies in non-human primate models of tuberculosis. *Immunol. Rev.* **264**(1), 60–73 (2015).
12. Carow, B. *et al.* Spatial and temporal localization of immune transcripts defines hallmarks and diversity in the tuberculosis granuloma. *Nat. Commun.* **10**(1), 1823 (2019).
13. Ehlers, S. & Schaible, U. The granuloma in tuberculosis: Dynamics of a host-pathogen collusion. *Front. Immunol.* **3**, 411. https://doi.org/10.3389/fimmu.2012.00411 (2013).
14. Koch, R. The etiology of tuberculosis. *Mittheilungen aus dem Kaiserlichen Gesundheitsamte.* **2**, 1–88 (1884).
15. Joosten, S. A. *et al.* Harnessing donor unrestricted T-cells for new vaccines against tuberculosis. *Vaccine* **37**(23), 3022–30 (2019).
16. Mattila, J. T., Diedrich, C. R., Lin, P. L., Phuah, J. & Flynn, J. L. Simian Immunodeficiency virus-induced changes in T cell cytokine responses in cynomolgus macaques with latent mycobacterium tuberculosis infection are associated with timing of reactivation. *J. Immunol.* **186**(6), 3527–3537 (2011).
17. Diedrich, C. R. *et al.* Reactivation of latent tuberculosis in cynomolgus macaques infected with SIV is associated with early peripheral T cell depletion and not virus load. *PLoS One* **5**(3), e9611 (2010).
18. Yao, S. *et al.* CD4 + T cells contain early extrapulmonary tuberculosis (TB) dissemination and rapid TB progression and sustain multieffector functions of CD8 + T and CD3 – lymphocytes: Mechanisms of CD4 + T cell immunity. *J. Immunol.* **192**(5), 2120–2132 (2014).
19. Gideon, H. P. *et al.* Variability in tuberculosis granuloma T cell responses exists, but a balance of pro- and anti-inflammatory cytokines is associated with sterilization. *PLoS Pathog.* **11**(1), 1–28 (2015).
20. Chen, C. Y. *et al.* A critical role for CD8 T cells in a nonhuman primate model of tuberculosis. *PLoS Pathog.* **5**(4), e1000392 (2009).
21. Cadena, A. M., Flynn, J. L. & Fortune, S. M. The importance of first impressions: Early events in mycobacterium tuberculosis infection influence outcome. *MBio* **7**(2), e00342 (2016).
22. Reiley, W. W. *et al.* ESAT-6-specific CD4 T cell responses to aerosol Mycobacterium tuberculosis infection are initiated in the mediastinal lymph nodes. *Proc. Natl. Acad. Sci. U S A.* **105**(31), 10961–10966 (2008).
23. Gallegos, A. M., Pamer, E. G. & Glickman, M. S. Delayed protection by ESAT 6specific effector CD4+ T cells after airborne M. tuberculosis infection. *J. Exp. Med.* **205**(31), 2359–68 (2008).
24. Matzinger, P. The evolution of the danger theory. Interview by Lauren Constable commissioning editor. *Expert Rev. Clin. Immunol.* **8**(4), 311–7 (2012).
25. Andrews, J. R. *et al.* Risk of progression to active tuberculosis following reinfection with Mycobacterium tuberculosis. *Clin. Infect. Dis.* **54**(6), 784–791 (2012).
26. Clark, M. & Vynnycky, E. The use of maximum likelihood methods to estimate the risk of tuberculous infection and disease in a Canadian first nations population. *Int. J. Epidemiol.* **33**(3), 477–484 (2004).
27. Vynnycky, E. & Fine, P. E. M. The natural history of tuberculosis: The implications of age-dependent risks of disease and the role of reinfection. *Epidemiol. Infect.* **119**(2), 183–201 (1997).
28. Sutherland, I., Švandová, E. & Radhakrishna, S. The development of clinical tuberculosis following infection with tubercle bacilli. 1. A theoretical model for the development of clinical tuberculosis following infection, linking from data on the risk of tuberculous infection and the incidence of clinic. *Tubercle* **63**(4), 255–68 (1982).
29. Brooks-Pollock, E., Becerra, M. C., Goldstein, E., Cohen, T. & Murray, M. B. Epidemiologic inference from the distribution of tuberculosis cases in households in Lima Peru. *J. Infect. Dis.* **203**(11), 1582–1589 (2011).
30. Henao-Tamayo, M. *et al.* A mouse model of tuberculosis reinfection. *Tuberculosis* **92**(3), 211–217 (2012).
31. Repique, C. J., Li, A., Collins, F. M. & Morris, S. L. DNA immunization in a mouse model of latent tuberculosis: Effect of DNA vaccination on reactivation of disease and on reinfection with a secondary challenge. *Infect. Immun.* **70**(7), 3318–3323 (2002).
32. Cadena, A. M. *et al.* Concurrent infection with mycobacterium tuberculosis confers robust protection against secondary infection in macaques. *PLoS Pathog.* **14**(10), e1007305 (2018).
33. Sasson, S. C., Gordon, C. L., Christo, S. N., Klenerman, P. & Mackay, L. K. Local heroes or villains: Tissue-resident memory T cells in human health and disease. *Cell Mol. Immunol.* **17**(2), 113–22 (2020).

34. Scott, P. Long-lived skin-resident memory T cells contribute to concomitant immunity in cutaneous Leishmaniasis. *Cold Spring Harb. Perspect. Biol.* **12**(10), a038059 (2020).
35. Ogongo, P., Porterfield, J. Z. & Leslie, A. Lung tissue resident memory T-cells in the immune response to mycobacterium tuberculosis. *Front. Immunol.* **3**(10), 992 (2019).
36. Muruganandah, V., Sathkumara, H. D., Navarro, S. & Kupz, A. A systematic review: The role of resident memory T cells in infectious diseases and their relevance for vaccine development. *Front. Immunol.* **9**, 1574 (2018).
37. Darrah, P. A. *et al.* Prevention of tuberculosis in macaques after intravenous BCG immunization. *Nature* **577**(7788), 95–102 (2020).
38. Sershen, C. L., Plimpton, S. J. & May, E. E. Oxygen modulates the effectiveness of granuloma mediated host response to mycobacterium tuberculosis: A multiscale computational biology approach. *Front. Cell Infect. Microbiol.* **6**, 6 (2016).
39. Kirschner, D., Pienaar, E., Marino, S. & Linderman, J. J. A review of computational and mathematical modeling contributions to our understanding of mycobacterium tuberculosis within-host infection and treatment. *Curr. Opin. Syst. Biol.* **3**, 170–85 (2017).
40. Cicchese, J. M., Dartois, V., Kirschner, D. E. & Linderman, J. J. Both pharmacokinetic variability and granuloma heterogeneity impact the ability of the first-line antibiotics to sterilize tuberculosis granulomas [Internet]. *Front. Pharmacol.* **45**(333), 458. https://doi.org/10.3389/fphar.2020.00333 (2020).
41. Pienaar, E. *et al.* Comparing efficacies of moxifloxacin, levofloxacin and gatifloxacin in tuberculosis granulomas using a multi-scale systems pharmacology approach. *PLoS Comput. Biol.* **13**(8), e1005650 (2017).
42. Pitcher, M., Bowness, R., Dobson, S., Eftimie, R. & Gillespie, S. Modelling the effects of environmental heterogeneity within the lung on the tuberculosis life-cycle. *J. Theor. Biol.* **506**, 110381 (2019).
43. Català, M. *et al.* Modelling the dynamics of tuberculosis lesions in a virtual lung: Role of the bronchial tree in endogenous reinfection. *Plos Comput. Biol.* **16**(5), e1007772 (2020).
44. Wigginton, J. E. & Kirschner, D. A model to predict cell-mediated immune regulatory mechanisms during human infection with mycobacterium tuberculosis. *J. Immunol.* **166**(3), 1951–1967 (2001).
45. Joslyn, L. R., Linderman, J. J. & Kirschner, D. E. A virtual host model of Mycobacterium tuberculosis infection identifies early immune events as predictive of infection outcomes. *J. Theor. Biol.* **539**, 111042 (2022).
46. Morris, S. E., Farber, D. L. & Yates, A. J. Tissue-resident memory T cells in mice and humans: Towards a quantitative ecology. *J. Immun.* **203**(10), 2561 (2019).
47. Ranjeva, S. L. *et al.* Recurring infection with ecologically distinct HPV types can explain high prevalence and diversity. *Proc. Natl. Acad. Sci. U S A* **114**(51), 13573–13578 (2017).
48. Chohan, B., Lavreys, L., Rainwater, S. M. J. & Overbaugh, J. Evidence for frequent reinfection with human immunodeficiency virus type 1 of a different subtype. *J. Virol.* **79**(16), 10701–8 (2005).
49. Snyder, M. E. *et al.* Generation and persistence of human tissue-resident memory T cells in lung transplantation. *Sci. Immunol.* **4**(33), 5581 (2019).
50. Hansen, S. G. *et al.* Prevention of tuberculosis in rhesus macaques by a cytomegalovirus-based vaccine. *Nat. Med.* **24**(2), 130–143 (2018).
51. Verver, S. *et al.* Rate of reinfection tuberculosis after successful treatment is higher than rate of new tuberculosis. *Am. J. Respir. Crit. Care. Med.* **171**(12), 1430–1435 (2005).
52. Uys, P. *et al.* The risk of tuberculosis reinfection soon after cure of a first disease episode is extremely high in a hyperendemic community. *Plos One* **10**(12), e0144487 (2015).
53. Joslyn, L. R. *et al.* Integrating non-human primate, human, and mathematical studies to determine the influence of BCG timing on H56 vaccine outcomes. *Front. Microbiol.* **9**, 1734 (2018).
54. Marino, S., El-Kebir, M. & Kirschner, D. A hybrid multi-compartment model of granuloma formation and T cell priming in tuberculosis. *J. Theor. Biol.* **280**(1), 50–62 (2011).
55. Takamura, S. & Kohlmeier, J. E. Establishment and maintenance of conventional and circulation-driven lung-resident memory CD8+ T cells following respiratory virus infections. *Front. Immunol.* **10**, 733 (2019).
56. Slütter, B. *et al.* Dynamics of influenza-induced lung-resident memory T cells underlie waning heterosubtypic immunity. *Sci. Immunol.* **2**(7), eaag2031 (2017).
57. Campbell, D. B. Can allometric interspecies scaling be used to predict human kinetics?. *Drug Inf. J.* **28**(1), 235–45 (1994).
58. de Boer, R. J. & Perelson, A. S. Quantifying T lymphocyte turnover. *J. Theor. Biol.* **327**, 45–87 (2013).

Acknowledgements

Author contributions

L. J. performed the modeling study analysis, J. F provide datasets and relevant biological input, D. K. and J. L. conceptualized the model and oversaw all aspects of its development. All authors contributed to the writing of the paper.

Competing interests

The authors declare no competing interests.

Additional information

Supplementary Information The online version contains supplementary material available at https://doi.org/10.1038/s41598-022-24516-8.

Correspondence and requests for materials should be addressed to D.E.K. or J.J.L.

Reprints and permissions information is available at www.nature.com/reprints.

Publisher's note Springer Nature remains neutral with regard to jurisdictional claims in published maps and institutional affiliations.